

Microcavities with suspended subwavelength structured mirrors

Andreas Naesby¹ and Aurélien Dantan^{1,*}

¹*Department of Physics and Astronomy, University of Aarhus, DK-8000 Aarhus C, Denmark*

(Dated: May 18, 2022)

We investigate the generic properties of optical cavities with subwavelength structured mirrors whose reflectivity profile exhibit Fano resonances. We focus in particular on short microcavities and mirrors with high quality factor Fano resonances for which the cavity free-spectral range becomes larger than the width of the Fano resonance. In this unusual regime, the transmission spectrum of the microcavity essentially consists in a single mode, whose linewidth can be substantially reduced as compared to both the Fano resonance width and the linewidth of an equally short cavity without structured mirror. The robustness of these narrow transmission features with respect to wavefront curvature and imperfect parallelism effects suggests that such microcavities could be realized in practice using suspended structured thin films in a simple plane-parallel geometry, and could have interesting applications for optomechanics and sensing applications.

Interference effects in structured thin films are widely exploited in photonics to tailor the properties of integrated optical elements. Of particular interest are thin films patterned with subwavelength structures, such as high-contrast gratings [1] or photonic crystals [2]. There, interference between modes propagating through the film and transverse guided modes result in the appearance of Fano resonances [3], which can bring about remarkable optical properties, such as broadband high-reflectivity or transmittivity, or the appearance of high quality factor resonances. Such features can be exploited for realizing a wide range of integrated photonics components, e.g., optical filters [4], couplers [5], reflectors [6], lasers [7], detectors [8], sensors [9], etc.

While such subwavelength structured films inherently display Fabry-Perot-type interferences [10], they are typically integrated with standard optical elements, e.g. in linear Fabry-Perot resonator configurations in order to enhance their spectral selectivity, detection sensitivity, or the strength of the light-matter interaction [1–3].

In this Letter, we investigate microcavities with suspended subwavelength structured mirrors and focus in particular on the regime in which the microcavity free-spectral range is larger than the width of a Fano resonance of the highly reflecting structured mirror. In this unusual regime, the transmission spectrum of the microcavity essentially consists in a single mode, whose linewidth can be significantly narrower than either the Fano resonance linewidth or the linewidth of an equally short cavity without structured mirror. We show for instance that few-micron long resonators with a Fano mirror with a moderately high Q resonance of a thousand and having finesse of a few hundreds at μm wavelengths can display GHz-wide transmission features. This generic interference effect occurring in any Fabry-Perot resonator with a strongly wavelength-dependent mirror could thus be exploited to enhance the spectral resolution of microcavities without increasing their modevolume [11]. Furthermore, these remarkably narrow linewidths are shown to be reasonably robust with respect to wavefront curvature and imperfect parallelism effects, so that such microcavities could be realized in practice

in a plane-parallel geometry, without resorting to optical elements with short focusing abilities [12–15]. The combination of ultrashort cavities with low-mass and high-mechanical quality *suspended* structured thin films [16–20] would be particularly interesting for optomechanics [19, 21–23] and sensing [15, 24] applications. Furthermore, realizing such microcavities by integrating the structured mirror in a fiber-optic Fabry-Perot interferometer would be an interesting alternative to fiber sensors with in-fiber embedded Bragg gratings [25].

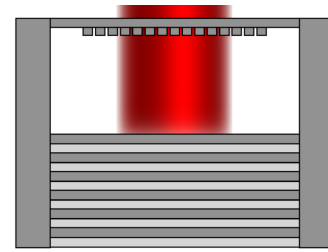


FIG. 1. Schematic of a microcavity consisting of a suspended Fano mirror (HCG) and a highly reflecting Bragg mirror.

Idealized 1D model – We start by considering an idealized one-dimensional scattering model, in which the optical resonator consists of two parallel, absorption-free mirrors (fig. 1): a highly reflecting mirror with amplitude transmission and reflection coefficients r and t , and a “Fano” mirror, whose reflection and transmission coefficients result of the interference between the direct transmission through the slab and a guided transverse mode [26, 27]

$$r_g(\omega) = i \frac{t_d \gamma + r_d(\omega - \omega_0)}{\gamma + i(\omega - \omega_0)}, \quad t_g(\omega) = \frac{r_d \gamma - t_d(\omega - \omega_0)}{\gamma + i(\omega - \omega_0)}, \quad (1)$$

where t_d and r_d are the normal incidence transmission and reflection coefficients, and γ the width of the transverse guided resonance mode with frequency ω_0 . This coupled-mode model is known to accurately reproduce the Fano resonances typically observed with subwavelength high-contrast grating (HCG) or photonic crystal structures [2, 3], and can thus be used as a simple basis to discuss the physics of Fano mirror resonators. For convenience, we start by modelling the mirrors as infinitely thin 1D scatterers, characterized by their

* Corresponding author: dantan@phys.au.dk

polarizabilities $\zeta = -ir/t$ and $\zeta_g(\omega) = -ir_g(\omega)/t_g(\omega)$, respectively. We assume that the highly-reflecting mirror polarizability ζ does not significantly vary over the frequency range of interest, while the frequency dependence of $\zeta_g(\omega)$ is prescribed by eq. (1). Denoting by l the cavity length, the overall transmission of the optical resonator is then given by

$$\mathcal{T} = \left| \frac{tt_g(\omega)}{1 - rr_g(\omega)e^{i2\omega l/c}} \right|^2. \quad (2)$$

To simplify the discussion we assume that the cavity length l is chosen such that the guided mode resonance frequency ω_0 coincides with one of the bare optical cavity resonance frequencies, satisfying $\omega_0 = (c/2l)(2\pi p + \arctan(1/\zeta))$, with p an integer and c the speed of light in vacuum. We also assumed r_g and t_g real for simplicity, and take $\zeta(\omega_0) \sim \zeta$ in order to mimic a symmetric cavity.

Depending on the ratio of the free spectral range $\gamma_{\text{FSR}} = c/(2l)$ and the width of the subwavelength structured mirror resonance γ , two regimes can be considered. Typically, “long” cavities and mirrors with relatively broad Fano resonances and $\gamma_{\text{FSR}} \ll \gamma$ and exhibit, within the bandwidth of the Fano resonance, Lorentzian cavity resonances with a linewidth given by the “bare” cavity linewidth $\kappa = \gamma_{\text{FSR}}/\pi\zeta^2$ (for $\zeta \gg 1$). By the “bare” cavity we refer here to a cavity having the same length, but for which both mirrors have a frequency-independent polarizability ζ . This regime is illustrated in Fig. 2a for a $\sim 200 \mu\text{m}$ -long cavity consisting of a highly reflecting mirror with $|r|^2 = 0.99$ and a Fano mirror with an optical resonance around 940 nm having a Q -factor of 20, resulting in a ratio $\gamma = 5\gamma_{\text{FSR}}$. The spectrum indeed exhibits cavity modes with linewidth κ around the Fano mirror resonance, while modes with larger linewidth and lower peak transmission are observed away from ω_0 due to the decrease in reflectivity of the Fano mirror.

However, for a short enough cavity, such that $\gamma_{\text{FSR}} \gg \gamma$, the cavity spectrum consists in one mode only, having a resonance frequency close to ω_0 . Remarkably, the linewidth of this mode can be much narrower than both the bare cavity linewidth κ and the Fano mirror resonance width γ . Assuming $\zeta_g(\omega_0) = \zeta \gg 1$, the transmission around resonance can be shown to be approximately given by

$$\mathcal{T}(\delta) \simeq \frac{1}{1 + F \left(\frac{\delta}{1-\zeta\delta} \right)^2}, \quad (3)$$

where $\delta = (\omega - \omega_0)/\gamma$ and $F \simeq \zeta^4$ is the coefficient of finesse of the bare cavity. The resulting Fano resonance profile displays a linewidth γ/\sqrt{F} , which is narrower than that of the Fano mirror by a factor given by the coefficient of finesse of the cavity. This effective narrowing in presence of the highly-reflecting cavity mirror can be understood by realizing that, even though the Fabry-Perot resonator only possesses one resonant mode, constructive interference occurs only for photons whose frequency detuning after $\sim \sqrt{F}$ roundtrips from the Fano resonance frequency is less than γ . Figure 2b shows the transmission of an $8.5 \mu\text{m}$ -long cavity with a Fano mirror with $Q \sim 10^3$, such that $\gamma = \gamma_{\text{FSR}}/100$. The resulting transmission linewidth is $\sim 10 \text{ pm}$, substantially narrower than the

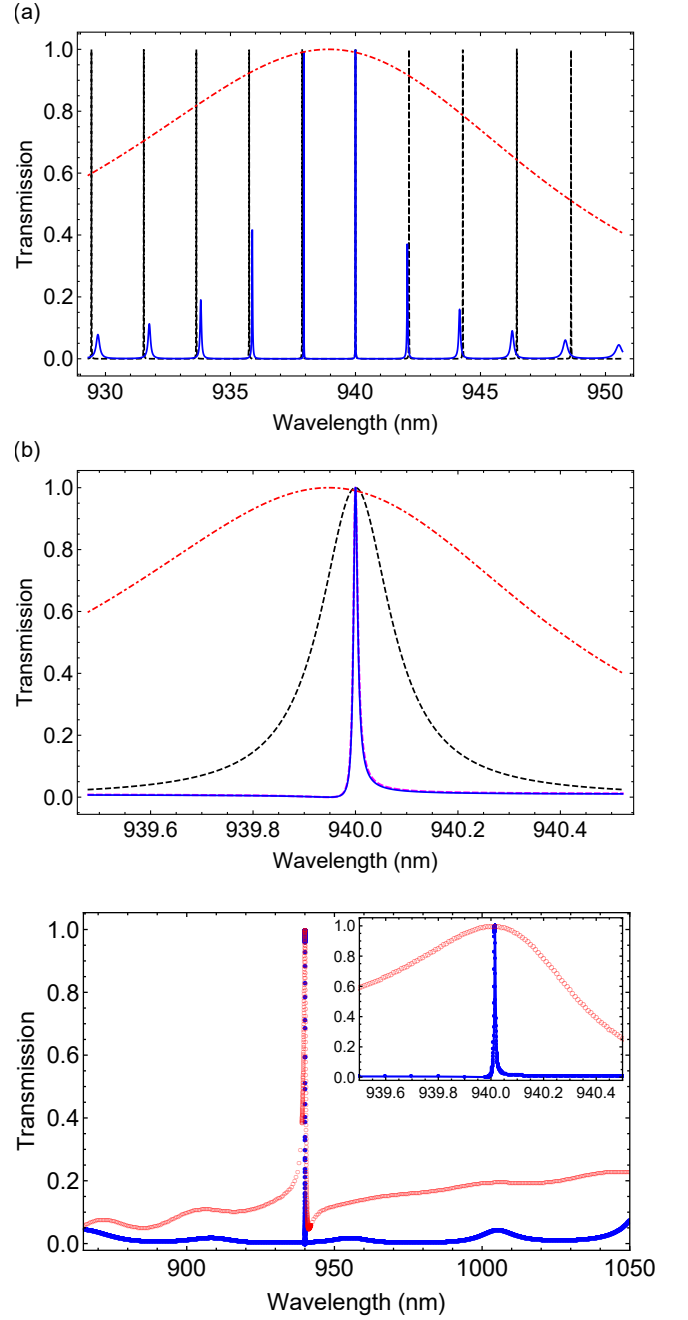


FIG. 2. Transmission spectrum of (a) $206.8 \mu\text{m}$ -long resonator with low- Q Fano mirror resonance of 21.3 ($\gamma = 5\gamma_{\text{FSR}}$) and (b) $8.5 \mu\text{m}$ -long resonator with high- Q Fano mirror resonance of 900 ($\gamma = \gamma_{\text{FSR}}/100$). Parameters: $|r|^2 = |t_d|^2 = 0.99$, $\lambda_0 = 2\pi c/\omega_0 = 940 \text{ nm}$. The plain blue curves show the results of the transfer matrix calculations, while the dashed red and dashed-dotted black curves show the Fano mirror reflectivity $|r_g|^2$ and the bare cavity spectrum, respectively. The dashed magenta curve in (b) shows the result of eq. (3). (c) Full-numerical simulation of the transmission spectrum of a Fano cavity (blue dots) consisting of a HCG and a Bragg mirror with parameters similar to (b). The red circles show the HCG reflectivity and the inset a zoom around the 6 pm (2 GHz)-wide resonant transmission line.

bare cavity linewidth of 0.26 nm and the Fano mirror width of 1.04 nm, and its profile is seen to be accurately reproduced by eq. (3).

Full 1D model – In order to confirm the findings of the infinitely thin scatterer model we numerically simulate the transmission spectrum of a cavity similar to that of Fig. 2b, consisting in a HCG and a multilayer Bragg mirror as in Fig. 1. We base ourselves on the subwavelength grating structures patterned on suspended silicon nitride films [16, 22], but note that similar results could readily be obtained with photonic crystal structures [15, 17–20, 28]. We consider a 200 nm-thick silicon nitride slab (refractive index $n = 2.0$), in which a high contrast grating with a period of 779 nm and 705 nm-wide, 50 nm-deep rectangular grating fingers is etched, in combination with a Bragg mirror consisting in 18 alternate layers of SiO_2 ($n = 1.455$) and Ta_2O_5 ($n = 2.041$) with $\pi/2$ thickness, and simulate the field propagation using the finite element modeling software Comsol using periodic Floquet boundary conditions. In this way, we realistically simulate a Fano mirror and a highly-reflecting mirror with parameters close to those of Fig. 2b. For a cavity length of $8.59 \mu\text{m}$, a ~ 6 pm-wide (~ 2 GHz) transmission line is obtained (Fig. 2c), thus supporting the previous analysis. Let us also point out that the numbers chosen in this example for the reflectivity level (99%) and optical quality factor (10^3) of the Fano mirrors are quite realistic experimentally [16, 19]. Substantially narrower linewidths could in principle be obtained, were one to use even more reflecting mirrors [20, 22] and/or ultrahigh- Q Fano resonances [4, 9].

Transverse effects – We now address effects going beyond the 1D scenario and start by investigating the effect of the incoming field transverse wavefront on the microcavity linewidth. For perfectly parallel plane mirrors, taking the wavefront curvature into account sets a fundamental limit to the achievable finesse and linewidth of the resonator. Such wavefront effects are particularly relevant for Fano mirrors whose structured area is relatively small, thus constraining the incoming beam size to avoid diffraction losses and, thereby, increasing the beam divergence inside the microcavity. For the sake of concreteness we assume an incoming Gaussian TEM_{00} mode having its waist w_0 at the Fano mirror. We take w_0 to be much smaller than the structured area in order to neglect trivial diffraction effects. Under these assumptions the outgoing field amplitude after the highly reflecting mirror is given by an infinite sum of reflected components

$$E(r, l) = \sum_n t_g (r r_g)^n e^{ikz_n} \exp\left(-\frac{r^2}{w(z_n)^2}\right) \times \exp\left[ik\frac{r^2}{2R(z_n)} - i\psi(z_n)\right] \frac{\sqrt{2/\pi}}{w(z_n)}, \quad (4)$$

where $k = 2\pi/\lambda$, $z_n = (1 + 2n)l$, $R(z) = z[1 + (z_R/z)^2]$, $z_R = \pi w_0^2/\lambda$, $w(z) = w_0 \sqrt{1 + (z/z_R)^2}$ and $\psi(z) = \arctan(z/z_R)$ are the standard Gaussian beam parameters. The relative transverse dephasing and reduction in reflectivity, which increase for each roundtrip, will obviously lead to a broadening of the spectrum and reduced cavity transmission, as compared to those observed in the idealized 1D plane-wave model. The

normalized cavity transmission $\mathcal{T} = \int_0^\infty |E(r, l)|^2 2\pi r dr$ is plotted on Fig. 3 for the same cavities as in Fig. 2 and for two different waist sizes of 20 and 50 μm . Figure 3a shows that the transmission of the long cavity is substantially broadened and reduced, even for the larger waist of 50 μm which corresponds to a Rayleigh range of 8 mm. In contrast, the linewidth of the short cavity is only slightly affected by wavefront curvature effects (Fig. 3b). This highlights another practical benefit of ultrashort Fano microcavities, for which ultranarrow transmission lines can be obtained even without resorting to Fano mirrors with focusing abilities [12–15].

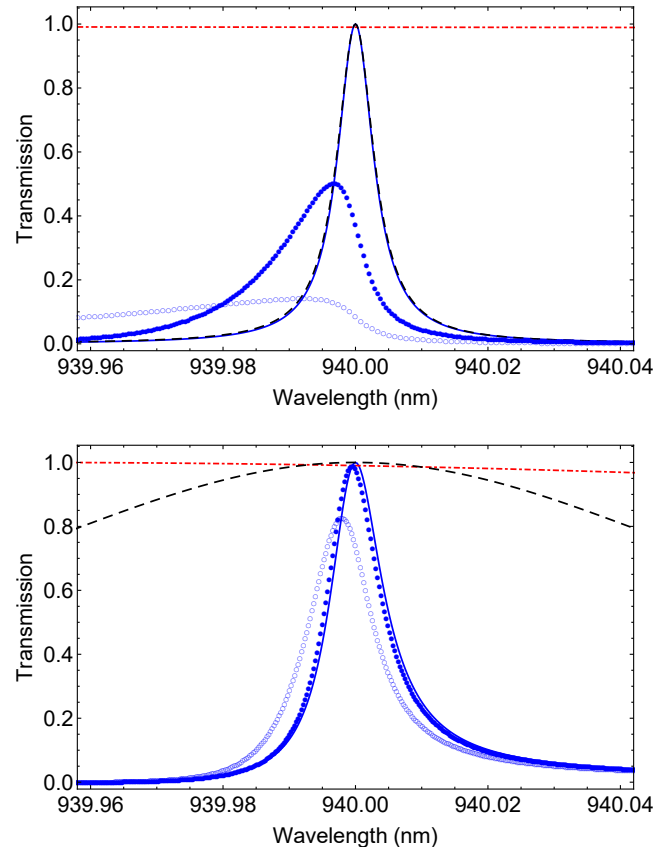


FIG. 3. (a) and (b): Transmission spectra of the cavities of Fig. 2a and 2b, respectively, taking into account the Gaussian wavefunction of the incoming light field. Plain (blue): plane wave case, full dots: $w_0 = 50 \mu\text{m}$, empty circles: $w_0 = 20 \mu\text{m}$. For reference, dashed (black): bare cavity spectrum, dash-dotted (red): Fano mirror reflectivity.

Another transverse effect worth investigating is the sensitivity of the microcavity linewidth with respect to imperfect parallelism between the mirrors. We still assume that the previous Gaussian mode impinges at normal incidence (z -direction) on the Fano mirror, but now the highly reflecting mirror makes an angle ϵ with the Fano mirror plane in the, say, x -direction. Following the approach of Ref. [29], geometrical considerations for the reflected field amplitudes lead to an outgoing field amplitude after the highly reflecting mir-

ror given by

$$E(x, y, l) = \sum_n t t_g (r r_g)^n E_n(x - x_n, y, l + z_n), \quad (5)$$

where $E_n(x, y, z) = E_{\text{in}}(x \cos(2n\epsilon), y, z + x \sin(2n\epsilon)) \sqrt{\cos(2n\epsilon)}$ is the field amplitude having experienced a wavefront tilt by $2n\epsilon$, $x_n = l / \tan(\epsilon) (1 / \cos(2n\epsilon) - 1)$ is the transverse walk-off of the n -th outgoing beam, $z_n = l \tan(2n\epsilon) / \tan(\epsilon)$ is the distance travelled by the n -th outgoing beam with reference to the direct transmission beam ($n = 0$). E_{in} is the incoming Gaussian modefunction at the Fano mirror. Figure 4 shows the resonance linewidth and resonant transmission levels of the previous $8.5 \mu\text{m}$ -long cavity with a $Q = 900$ Fano mirror resonance, for an incoming beam waist of $20 \mu\text{m}$ and for tilt angles which are achievable by, e.g., assembly of commercial silicon nitride membranes [30]. The linewidth broadening and resonant transmission reduction are consistent with the observation that, for small tilt angles, tilt-induced beam walkoff corrections scale as $F(\epsilon/\theta)^2$, where $\theta = \lambda/\pi w_0$ is the Gaussian beam divergence [30]. For a given degree of parallelism and cavity finesse, there generally exists an optimal waist size which minimizes the linewidth, as too large a beam increases the dephasing due to the tilt-induced beam walkoff, but too small a beam results in stronger wavefront effects. Let us finally note that these effects, in particular for high-finesse cavities, would be mitigated by the use of Fano mirrors with focusing abilities [12–15].

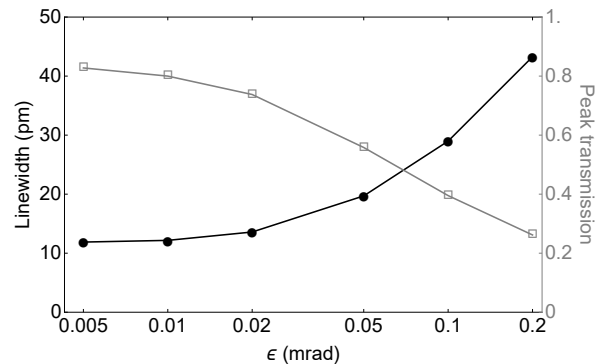


FIG. 4. Resonance linewidth (black dots) and resonant transmission level (gray squares) of an $8.5 \mu\text{m}$ -long cavity with a $Q = 900$ Fano mirror, for various tilt angles ϵ . $w_0 = 20 \mu\text{m}$ and $|r|^2 = |t_d|^2 = 0.99$. The lines are guides for the eyes.

To conclude, we investigated the generic transmission properties of a linear Fabry-Perot resonator incorporating a Fano mirror with a strongly wavelength-dependent reflectivity, such as can be realized with high-contrast gratings or two-dimensional photonic crystals. We showed in particular that enhanced spectral resolution can be achieved with ultrashort microcavities using suspended structured membranes in a simple parallel-plane geometry and for realistic parameters. Cavities with vibrating Fano mirrors would be particularly interesting as integrated devices for photonics and optomechanical sensors, and, if further combined with electrical actuation [31], for nano-electro-optomechanics [32].

Funding Information – The Velux Foundations.

-
- [1] C. J. Chang-Hasnain and W. Yang, *Adv. Opt. Photon.* **4**, 379 (2012).
- [2] W. Zhou, D. Zhao, Y.-C. Shuai, H. Yang, S. Chuwongin, A. Chadha, J.-H. Seo, K. X. Wang, V. Liu, Z. Ma, and S. Fan, *Progress in Quantum Electronics* **38**, 1 (2014).
- [3] A. E. Miroshnichenko, S. Flach, and Y. S. Kivshar, *Rev. Mod. Phys.* **82**, 2257 (2010).
- [4] Y. Shuai, D. Zhao, Z. Tian, J.-H. Seo, D. V. Plant, Z. Ma, S. Fan, and W. Zhou, *Opt. Express* **21**, 24582 (2013).
- [5] Y. Zhou, V. Karagodsky, B. Pesala, F. G. Sedgwick, and C. J. Chang-Hasnain, *Opt. Express* **17**, 1508 (2009).
- [6] F. Brückner, D. Friedrich, T. Clausnitzer, M. Britzger, O. Burmeister, K. Danzmann, E.-B. Kley, A. Tünnermann, and R. Schnabel, *Phys. Rev. Lett.* **104**, 163903 (2010).
- [7] M. C. Y. Huang, Y. Zhou, and C. J. Chang-Hasnain, *Nature Photonics* **1**, 119 (2007).
- [8] L. Chen, H. Yang, Z. Qiang, H. Pang, L. Sun, Z. Ma, R. Pate, A. Stiff-Roberts, S. Gao, J. Xu, G. J. Brown, and W. Zhou, *Applied Physics Letters* **96**, 083111 (2010).
- [9] Y. Zhou, M. Moewe, J. Kern, M. C. Y. Huang, and C. J. Chang-Hasnain, *Opt. Express* **16**, 17282 (2008).
- [10] V. Karagodsky, C. Chase, and C. J. Chang-Hasnain, *Opt. Lett.* **36**, 1704 (2011).
- [11] M. H. Bitarafan and R. G. DeCorby, *Sensors* **17**, 1748 (2017).
- [12] D. Fattal, J. Li, Z. Peng, M. Fiorentino, and R. G. Beausoleil, *Nature Photonics* **4**, 466 (2010).
- [13] A. B. Klemm, D. Stellinga, E. R. Martins, L. Lewis, G. Huyet, L. O’Faolain, and T. F. Krauss, *Opt. Lett.* **38**, 3410 (2013).
- [14] A. Arbabi, Y. Horie, A. J. Ball, M. Bagheri, and A. Faraon, *Nature Communications* **6**, 7069 (2015).
- [15] J. Guo, R. A. Norte, and S. Gröblacher, *Opt. Express* **25**, 9196 (2017).
- [16] U. Kemiktarak, M. Metcalfe, M. Durand, and J. Lawall, *Applied Physics Letters* **100**, 061124 (2012).
- [17] C. H. Bui, J. Zheng, S. W. Hoch, L. Y. T. Lee, J. G. E. Harris, and C. W. Wong, *Applied Physics Letters* **100**, 021110 (2012).
- [18] R. A. Norte, J. P. Moura, and S. Gröblacher, *Phys. Rev. Lett.* **116**, 147202 (2016).
- [19] C. Reinhardt, T. Müller, A. Bourassa, and J. C. Sankey, *Phys. Rev. X* **6**, 021001 (2016).
- [20] X. Chen, C. Chardin, K. Makles, C. Car, S. Chua, R. Braive, I. Robert-Philip, T. Briant, P.-F. Cohadon, A. Heidmann, T. Jacqmin, and S. Delglise, *Light: Science & Applications* **6**, e16190 (2017).
- [21] J. D. Thompson, B. M. Zwickl, A. M. Jayich, F. Marquardt, S. M. Girvin, and J. G. E. Harris, *Nature* **452**, 72 (2008).
- [22] U. Kemiktarak, M. Durand, M. Metcalfe, and J. Lawall, *New J. Phys.* **14**, 125010 (2012).

- [23] A. Xuereb, C. Genes, and A. Dantan, *Phys. Rev. Lett.* **109**, 223601 (2012).
- [24] A. Naesby, S. Naserbakht, and A. Dantan, *Applied Physics Letters* **111**, 201103 (2017).
- [25] M. R. Islam, M. M. Ali, M.-H. Lai, K.-S. Lim, and H. Ahmad, *Sensors* **14**, 7451 (2014).
- [26] S. Fan and J. D. Joannopoulos, *Phys. Rev. B* **65**, 235112 (2002).
- [27] S. Fan, W. Suh, and J. D. Joannopoulos, *J. Opt. Soc. Am. A* **20**, 569 (2003).
- [28] J. P. Moura, R. A. Norte, J. Guo, C. Schäfermeier, and S. Gröblacher, *Opt. Express* **26**, 1895 (2018).
- [29] J. Y. Lee, J. W. Hahn, and H.-W. Lee, *J. Opt. Soc. Am. A* **19**, 973 (2002).
- [30] B. Nair, A. Naesby, and A. Dantan, *Opt. Lett.* **42**, 1341 (2017).
- [31] S. Wu, J. Sheng, X. Zhang, Y. Wu, and H. Wu, *AIP Advances* **8**, 015209 (2018).
- [32] L. Midolo, A. Schliesser, and A. Fiore, *Nature Nanotechnology* **13**, 11 (2018).